JOURNAL OF MATERIALS SCIENCE **34** (1999) 3555–3564

Effect of microstructure on the mechanical properties and fracture of commercial hypoeutectic Al-Si alloy modified with Na, Sb and Sr

N. FATAHALLA, M. HAFIZ
Mechanical Department, Faculty of Engineering, Al Azhar University, Nasr City, Cairo, Egypt (Postal Code 11371)

M. ABDULKHALEK
Senior Engineer, Industrial Engineering Company for Construction and Development (ICON), Cairo, Egypt
E-mail: nfatahalla@frcu.eun.eg

The microstructure, hardness, tensile properties and fracture have been studied for the non-modified and modified aluminium (Al) silicon (Si) commercial hypoeutectic alloy. Three modifiers were used being sodium (Na), antimony (Sb) and strontium (Sr). The Sb-modified structure revealed small plate-like Si morphology. The Na and Sr-modified structures exhibited fibrous Si. A slight increase in the hardness values (HV) due to modification was observed. A general increase in the tensile properties was observed due to modification. The tensile properties of the sand mould Sr-modified alloy were significantly higher than those of the Na-modified alloy by 12.7% in proof stress, 16.3% in ductility and 33.3% in toughness. For the metal mould ingots the increase in tensile properties of Sr-modified alloy were respectively: 16.7%, 32.5% and 41.7% compared to a Na-modified alloy. Optical fractography on longitudinal sections near the fracture surfaces of the modified alloys revealed that the crack propagates in the eutectic thus, circumventing the Al-dendrites. The dimple and smooth ripple patterns observed by scanning electron microscope (SEM) on the fracture surface of the Na and Sr-modified alloys suggest a transgranular type of fracture across the grains of the eutectic matrix.

1. Introduction

In spite of the well-known [1] numerous advantages of Al-Si alloys and their widespread applications [2, 3], however, their use in industry as structural materials have been limited due to lack of ductility. The poor ductility refers to the microstructure, which contains plate-like Si particles, embedded in an Al-matrix. Considerable work has been done concerning the microstructural modification of Al-Si alloys. The modification process of these alloys has been carried out using several modifiers. The most widely used commercial modifiers are Na [4–8] and Sr [4, 7, 8, 10, and 13–20]. The numerous publications on modification pointed out that each of these modifiers has a beneficial influence on the structure of the eutectic. However, the choice of the best modifier in order to obtain parts having optimum properties seems to be still an open question.

In the present investigation an Al-5.5mass%Si alloy (commercially produced in Egypt for production of automobile pistons) was used as a reference material. The research aimed at retaining the good properties of this alloy (e.g. low density, relatively high strength and good wear resistance...) besides improving its ductility and consequently its toughness. The Na, Sb and Sr modifiers were selected to achieve this goal. The investigation implied studying the microstructure, hardness, tensile properties and fracture of the non-modified and modified-alloys. The effect of the three modifying processes on the properties of the investigated alloy is discussed. Correlation among microstructure, mechanical properties and fracture is presented.

2. Experimental

The chemical analysis of the reference material used is listed in Table I. The solidification cooling rates (SCRs) were measured using a chromel-alumel thermocouple connected to a digital counter and an x-t recorder. Table II presents the characteristics of the two types of moulds used to allow two distinct SCRs.

Firstly, the modification process with sodium was carried out by adding 1% of a mixture of Na-salts (two thirds of Na-fluoride and one third of Na-chloride) [14] to the molten metal. These salts were preheated to

TABLE I Chemical analysis of the reference material used in the present investigation

Element	Si	Mg	Fe	Cu	Mn	Ti	Ca	Al
Mass%	5.5	0.005	0.46	0.009	0.006	0.02	0.0037	Balance

Ni, Zn and Pb are almost nil.

TABLE II Type of mould and corresponding SCR

Type of mould	SCR (K/s)
Sand	0.6
Metal (steel)	16

523 K prior to adding to the molten metal at 1023 K. The melt was then superheated to 1053 K prior to pouring into sand and metal moulds. The melting operation was carried out in a vertical electric furnace connected with a millivolt device for controlling the temperature. The charges were melted in a steel-crucible lined with graphite and liquid glass. The crucible cavity-size was about 500 ml and the mass of the melt was 1250 g approximately.

Secondly, the Sb-treatment was performed by adding 0.8% of pure metal to the Al-Si alloy [9]. The Sb was added at 993 K and the molten metal was held for 300 s inside an electric furnace at 993 K and poured directly into the moulds.

Thirdly, modification was performed by adding 0.015%Sr in the form of extruded rods (9 mm diameter) of Al-5%Sr master alloy [16–19, 25, 26]. Small pieces were cut from the extruded rod for addition into the melt at 993 K. The molten metal was manually stirred for few seconds and then held, prior to casting, in the furnace at the same temperature of 993 K, to ensure homogeneity [27]. At the end of the holding period, the molten alloy was taken out of the furnace, skimmed and poured directly into sand and metal moulds.

Standard technique [28] was used for the metallographic study. Metallographic examination was carried out using the SEM after specimens had been deeply etched for 1.8 ks with a 5%NaOH solution. The volume fraction (VF) of the constituent phases has been detected using the point counting technique [29].

Macrohardness values were obtained using the Vickers test. A square-based pyramid indenter with an angle of 136° was used. A load of 15.625 kg was applied for a period of 30 s.

Standard tensile specimens were machined to gauge dimensions of 5 mm diameter and 25 mm length. The tensile tests were conducted on a motor driven tensometer type "W". Tensile tests were performed at ambient temperature of 300 K at a strain rate of $4 \times 10^{-4}\ s^{-1}$.

The tensile fracture characteristics were examined using both optical microscope and SEM. The optical microscope was used to investigate the longitudinal sections near the fractured surfaces. Additionally, the SEM was employed to reveal the fractography of the fractured surfaces.

3. Results

3.1. Microstructure

Fig. 1 shows the eutectic-Si size and morphology as revealed by the SEM of the non-modified alloy cast

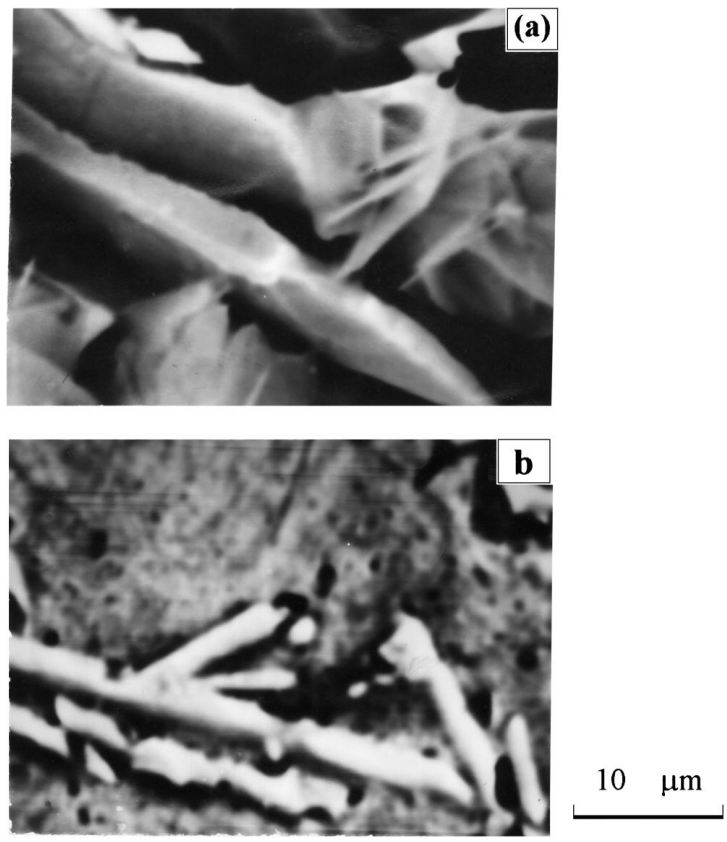

Figure 1 Effect of mould-type (solidification cooling rate) on the eutectic-Si size and morphology for nonmodified alloy; (a) sand mould and (b) metal mould.

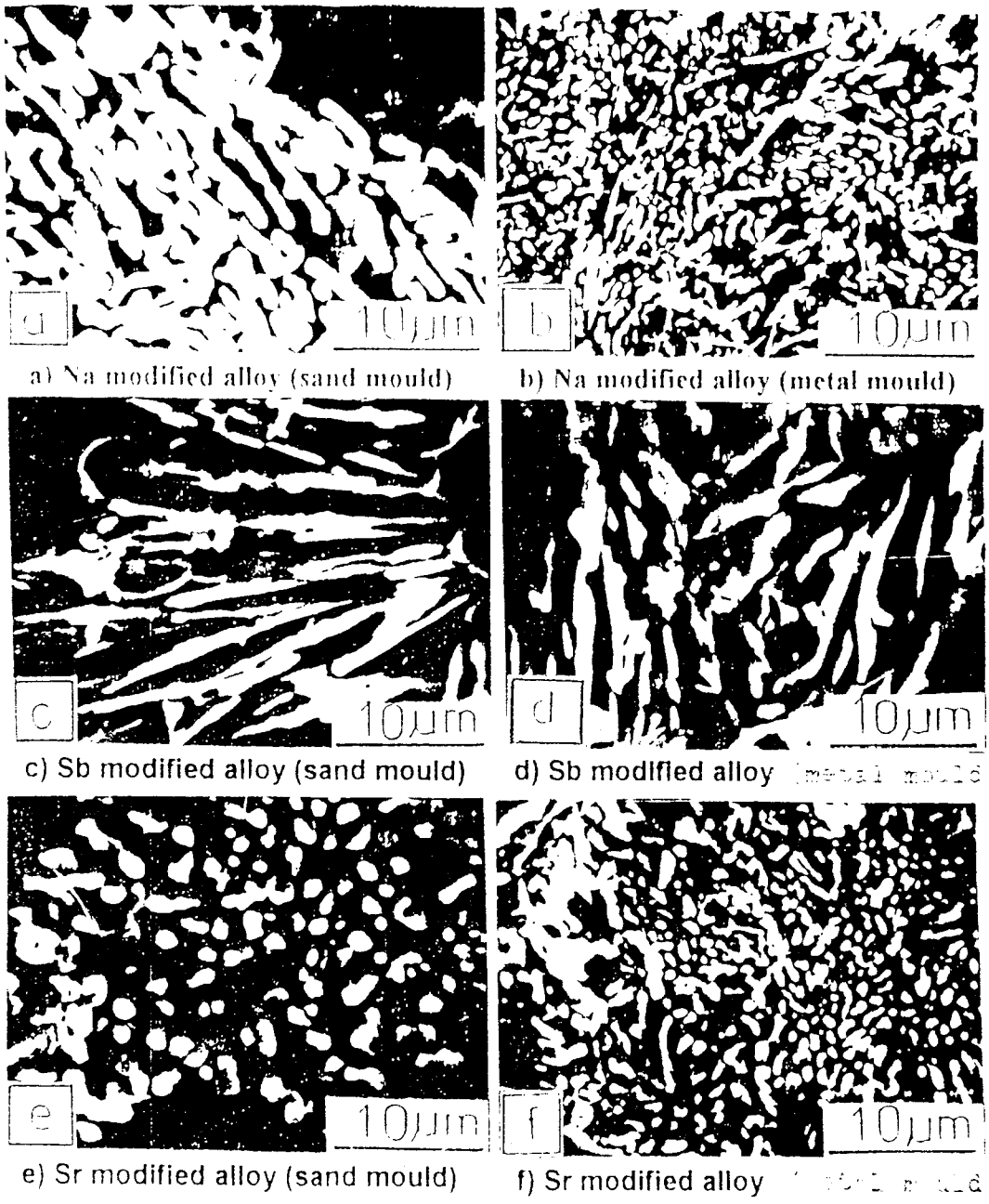

Figure 2 Silicon morphology of an Al-5.5%Si alloy modified respectively with Na, Sb and Sr.

into both sand and metal moulds. It can be seen that the eutectic-Si is of plate-like morphology. The dimensions of these platelets are indicative of the SCR. The effect of Na-modification on the Si-morphology is shown in Fig. 2a and b for both sand and metal mould cast ingots. The eutectic-Si shows, generally, a fibrous morphology. However, the size was smaller for the metal mould ingot (Fig. 2b) in comparison to the sand mould ingots (Fig. 2a).

A three dimensional observation of the Sb-modified alloy (Fig. 2c and d) exhibits a lamellar form of the eutectic-Si. Sb addition did not result in a fibrous Si morphology, as was the case with Na-modification.

The microstructure of the Sr-modified alloy is shown in Fig. 2e and f. Fibrous eutectic-Si morphology can be seen for both SCRs. This fibrous morphology resembles that of a Na-modified alloy (cf. Fig. 2a and b). However, in the case of Sr the Si-particles size was scaled down to finer fibres.

For an Al-5.5%Si binary alloy it can be determined from the equilibrium diagram [17] that the volume fraction of Al-solid solution (Vf_α) is 56%. The results obtained from the microstructures for the Vf_α are listed in Table III for both non-modified and modified alloys. A general increase in the values of Vf_α for the modified alloys can be observed. Additionally, it seems that the SCR plays also a role, which affects the value of Vf_α.

TABLE III Effect of Na, Sb and Sr modification and type of mould on the volume fraction of Al-solid solution

Alloy condition	Volume fraction of Al-solid solution (%)	
	Sand mould	Metal mould
Nonmodified	57	59
Na modified	59	60
Sb modified	58	59.6
Sr modified	60	61

TABLE IV Vickers hardness of non-modified and modified Al-5.5%Si alloy

Alloy condition	Vickers Hardness (MPa)	
	Sand mould	Metal mould
Non-modified	445	460
Na-modified	448	462
Sb-modified	468	475
Sr-modified	482	491

3.2. Hardness

The Vickers hardness values are given in Table IV for both the non-modified and modified alloys. A slight increase in hardness can be observed due to modification process. The hardness of the Sr-modified alloy reached the maximum value of all tested specimens (cf. Table IV). However, the hardness of the Sr-modified alloy increased only by about 8% for sand mould ingots and 6.7% for metal mould ingots in comparison with hardness of the respective non-modified ingots.

3.3. Tensile properties

Table V lists the results of the tensile test for both modified and non-modified alloys. The 0.2% proof stress (σ_{pr}), ultimate tensile strength (UTS), elongation percent (E%) and toughness, which is defined by the area under the engineering stress-strain diagram, were the tensile properties under consideration. It should be noted that the modification processes have, generally, improved the mechanical properties (strength, ductility and toughness) relative to the non-modified alloy.

The Sr-modified alloy showed the highest properties, followed by Na-modified one, and thirdly the Sb-modified alloy. σ_{pr} of the Sr-modified alloy cast in sand mould (62 MPa) represents 168% of the value for the non-modified alloy (37 MPa). It is also higher than σ_{pr} of the alloy modified with Na (55 MPa) and Sb (50 MPa). Additionally, the UTS of the Sr-modified alloy (124 MPa) is approximately 168% of the value for the non-modified alloy. Likewise, the UTS of the Sr-modified alloy is higher than that for the Na-modified (114 MPa) and for Sb-modified (115 MPa). Naturally, the UTS of the Sr-modified alloy was 168% of the value for the non-modified alloy (74 MPa). On the other hand, a more pronounced effect of modification was observed on the ductility of the investigated Al-Si alloy. The ductility of the Sr-modified alloy reached a value of 5% which is 3 to 4 times the value for non-modified alloy (1.4%) and, in addition to that, it is higher than the ductility of the Na-modified alloy (4.3%) and Sb-modified alloy (3.7%). In consistence with strength and ductility results the toughness of the Sr-modified alloy (5.2 MPa) was superior to values for non-modified alloy (0.95 MPa), Na-modified alloy (3.9 MPa) and Sb-modified alloy (3.7 MPa).

By analogy, the tensile properties of the metal mould ingots resembled those explained in the previous paragraph for the sand mould ingots. The σ_{pr}, UTS, E% and toughness of the Sr-modified alloy showed the highest values (70 MPa, 142 MPa, 10.6% and 11.9 MPa respectively), Na-modified (60 MPa, 96 MPa, 2.5% and 2 MPa respectively) and Sb-modified (56 MPa, 115 MPa, 7.3% and 7.4 MPa respectively).

It should be indicated here that the increase in the mechanical properties (under consideration) due to modification, which is higher for the metal mould ingots, compared to sand mould ingots. The higher SCR appears to be the main reason.

3.4. Fracture characteristics

As has been previously indicated [18], the examination by the optical microscopy of the longitudinal section near the fracture surfaces of the non-modified alloys cast in both sand and metal moulds revealed an intergranular mode of fracture passing along the eutectic ribbon around the α-particles. Fig. 3a–f shows the longitudinal section near the fracture surfaces of the alloys modified with Na (Fig. 3a and b), Sb (Fig. 3c and d) and Sr (Fig. 3e and f). In Fig. 3, it is a general feature that the fracture paths are propagating along the eutectic phase circumventing the relatively ductile Al-solid solution dendrites. However, it is not clear from Fig. 3 whether this fracture path propagates transgranularly or intergranularly in the interior of the eutectic matrix. This will be more clearly demonstrated by SEM observations.

Fractographs showing the fracture surfaces of the non-modified alloy are given in Fig. 4a and b. The similarity between these photographs gives the impression that the variation in the SCR did not have an impact on the fracture process of the non-modified alloy. Apparently, Si-particles occupy a considerable

TABLE V Effect of solidification cooling rate (type of mould) and Na, Sb and Sr-modification on the tensile properties of non-modified and modified Al-5.5%Si alloy

Alloy condition	Mould type	Tensile properties			
		$\sigma_{pr\,(MPa)}$	UTS (MPa)	E%	Toughness (MPa)
Non-modified	Sand mould	37	74	1.4	0.95
	Metal mould	48	96	2.5	2.0
Na-modified	Sand mould	55	114	4.3	3.9
	Metal mould	60	121	8.0	8.4
Sb-modified	Sand mould	50	109	3.7	3.7
	Metal mould	56	115	7.3	7.4
Sr-modified	Sand mould	62	124	5.0	5.2
	Metal mould	70	142	10.6	11.9

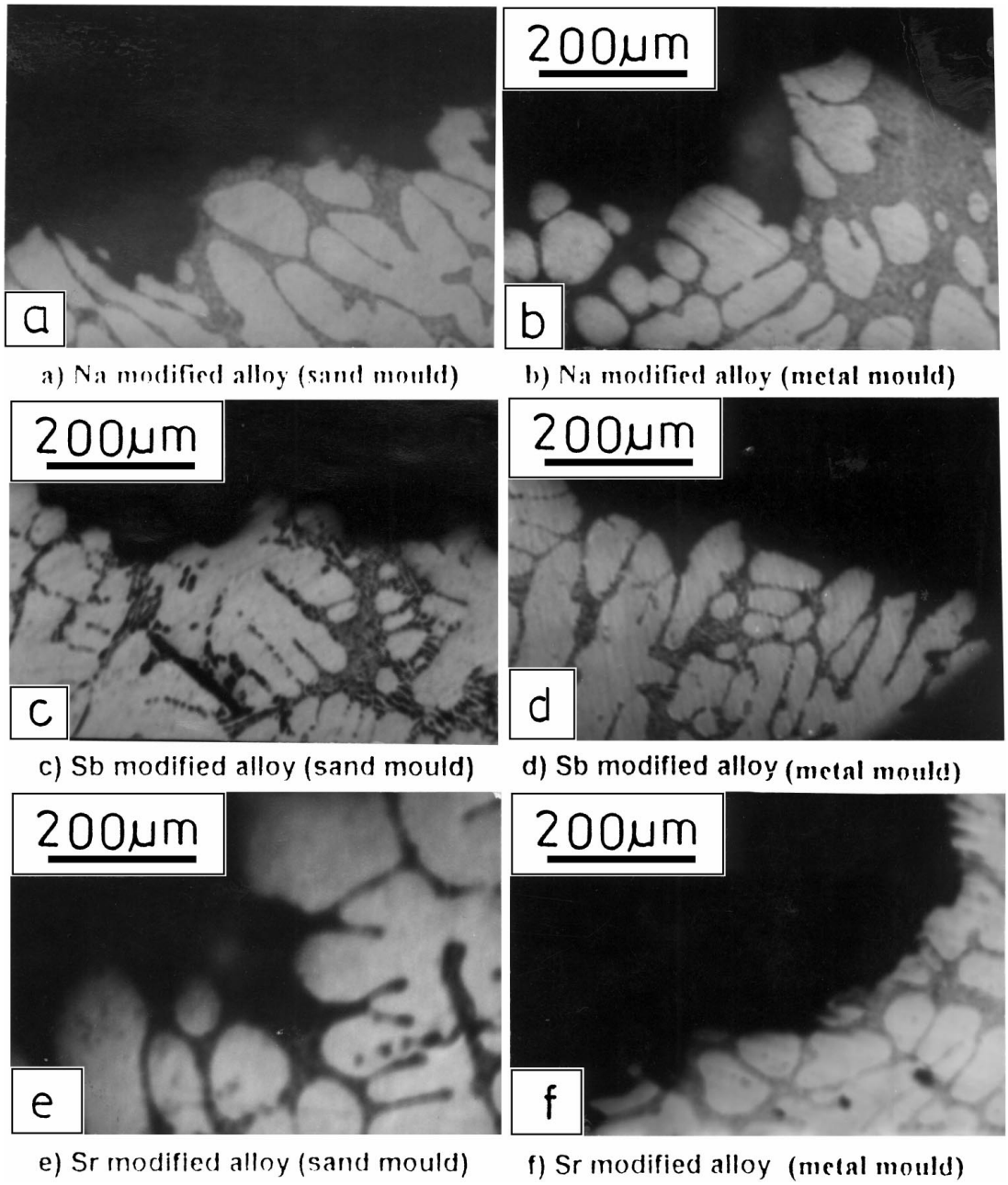

Figure 3 Longitudinal section near the fracture surfaces of modified-alloys.

portion of the fracture surfaces in Fig. 4. A broken eutectic-Si is the characteristic of the fracture surface of both sand and metal mould cast specimens. Broken Si-particles could be detected on the fracture surfaces, as indicated by area "*A*" in Fig. 4a. It should also be noted that no separation of Si-particles from the matrix was observed. The features of Fig. 4 are typical of brittle fracture [16 and 17].

Fig. 5a and b shows the effect of Na addition on the fracture characteristics of the alloy. It can be seen that the form of the Si-particles of the Na-modified alloy has a significant effect on the fracture process. Ripple pattern of fracture can be observed on the fracture surface. A broken Si-particle indicated by an arrow is observed in Fig. 5b.

Typical SEM fractographs of Sb-modified alloy are shown in Fig. 5c and d. These fractographs exhibit a mixed mode of fracture. The fracture surface is characterised by areas of typical ductile fracture and others show cleavage-type of fracture. However, both types of fracture are dominated by the eutectic-Si particles.

Fractographs showing the fracture surfaces of Sr-modified alloy cast into sand and metal moulds are given in Fig. 5e and f. Regardless of the SCR, two features characterise the fracture surfaces of Sr-modified alloy being dimple and ripple pattern of fracture. It is interesting to note that the dimples of metal mould cast ingots are shallower and larger than those of sand mould cast ingots.

4. Discussion

4.1. Microstructure

In accordance with the results obtained previously by the present authors [16–27], the microstructure of the non-modified sand mould ingot revealed, generally, coarse dendrites and eutectic structure. This phenomenon could be seen by the optical microscopy

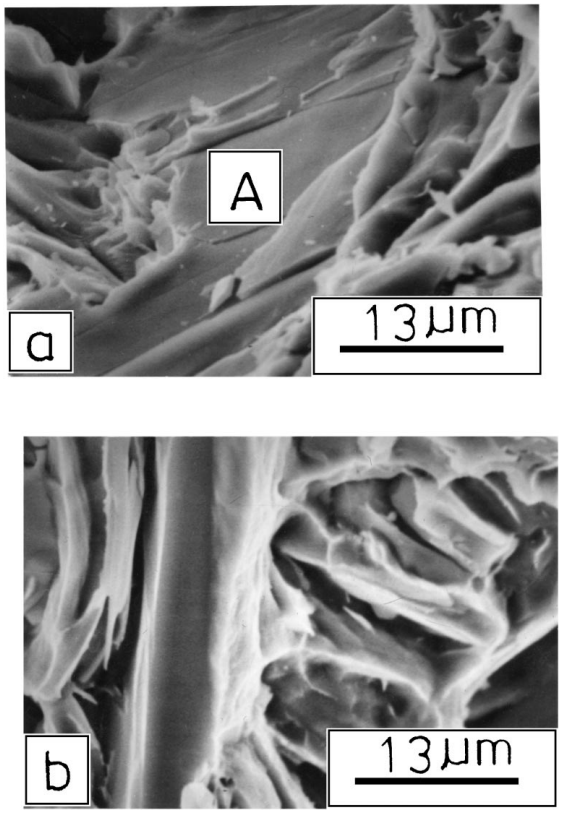

Figure 4 Features of the fracture surfaces of the nonmodified alloy as revealed by SEM (a) sand mould, and (b) metal mould.

previously [16, 17] and can be seen by the SEM in the present study (Fig. 1a) which reveals thick plate-like Si-morphology. The Si-platelets were smaller in the case of fast SCR (Fig. 1b). Therefore, it seems that SCR, in the domain of variation considered here, controls the structure refinement but it does have an impact on the morphology of eutectic-Si particles [22, 30].

The effect of Na-addition on the microstructure of the alloy is shown in Fig. 2a and b. The change in the morphology of Si-particles from plate-like to fibrous is achieved at both SCRs. The Si-particle size was found to be smaller for the metal mould ingots than that for its counterpart cast into sand mould. This is clearly observed by comparing Fig. 2a and b. The similarity of the Si-morphology between sand and metal mould cast of Na-modified alloy maybe explained in terms of the effect of Na on the nucleation and growth of Si [31, 32]. The similarity in the Si-particle size can only be due to the difference in the SCR. It is therefore, concluded that the application of high SCR in conjunction with Na-addition results in Si-particles which are significantly smaller than those obtained either by modification or by high SCR.

Sb is observed to have a different effect on the eutectic-Si than Na does (Fig. 2a and b). This lamellar structure (Fig. 2c and d) is finer than the eutectic structure in non-modified alloy. Thus, it is believed that Sb has a refinement effect on the microstructure rather than a modifying effect. The refining action of Sb is not as pronounced as the Na-modifying effect.

Fibrous-Si morphology was obtained after modification of the alloy with Sr as shown in Fig. 2e and f. The morphology of Si-particles is similar to a Na-modified alloy (Fig. 2a and b). This result implies that Sr can be considered as an alternative modifier to Na. It can also be noticed that the eutectic-Si particles in the Sr-modified alloy are much finer than that of both Na and Sb modified microstructure (Fig. 2a–f).

4.2. Volume fraction

The Al-Si phase diagram represents an ideal case, where phase transformations are allowed to take place infinitely slowly where as in casting transformations take place at finite rates. In most binary Al-Si alloys the deviation from the equilibrium eutectic temperature is a few degrees Kelvin [33, 34]. Therefore, during solidification the primary Al-solid solution grows quickly into the liquid. Thus, the liquid composition moves down following the liquidus line until the point of Si nucleation. This point is dependent on the SCR and the corresponding undercooling. As a consequence, more primary Al-solid solution is found in the metal mould cast alloy than in a similar alloy cast into sand mould (Table III). This result confirms the suggestion that the high SCR shifts the eutectic point to the right side of the phase-diagram, i.e. higher Si levels [35, 36].

Using thermal analysis [5], Radhakrishna showed that the modified alloy solidification temperature is lower than that of a non-modified one. Consequently, the eutectic-point is shifted to a higher Si level [37]. The new location of the eutectic-point is somewhere on the extension of the liquidus line, depending on the amount of the modifier and the SCR [37].

It is interesting to note that a higher amount of the Al-solid solution is the characteristic of the Sr-modified alloy, especially if cast in a metal mould. On the other hand, the values obtained for the Sb-modified alloy were, for both SCRs, lower. This maybe attributed to the relative amount of undercooling associated with each modifier. Therefore, the effectiveness of each modifier used resulting in the displacement of the eutectic-point towards a higher Si-content is in the following order: Sb, Na and Sr. Fig. 6 shows the location of the eutectic-point based on the Vf of the constituent-phases given in Table III.

4.3. Hardness

The slight increase in hardness with an increase in the SCR (Table IV) can be attributed to the microstructure refinement. Recalling that the microstructure of the present alloy comprises Al-solid solution and binary Al/Si eutectic (Si-particles embedded in Al-matrix). It is well known that Si-phase is harder than Al-phase. Thus, the size, morphology and distribution of the Si-particles could affect the hardness of the eutectic-mixture. Consequently, the hardest alloy should have a microstructure in which fine and uniformly distributed Si-particles are present in the Al-matrix. Such microstructure seems to be obtained in the case of Sr-modified alloy (Table IV). These results given in Table IV are confirmed by Mondolfo [38] in his report about the effect of modification on the hardness of some Al-Si alloys having Si-contents ranging from 5 to 7% by weight. His non-modified alloys showed

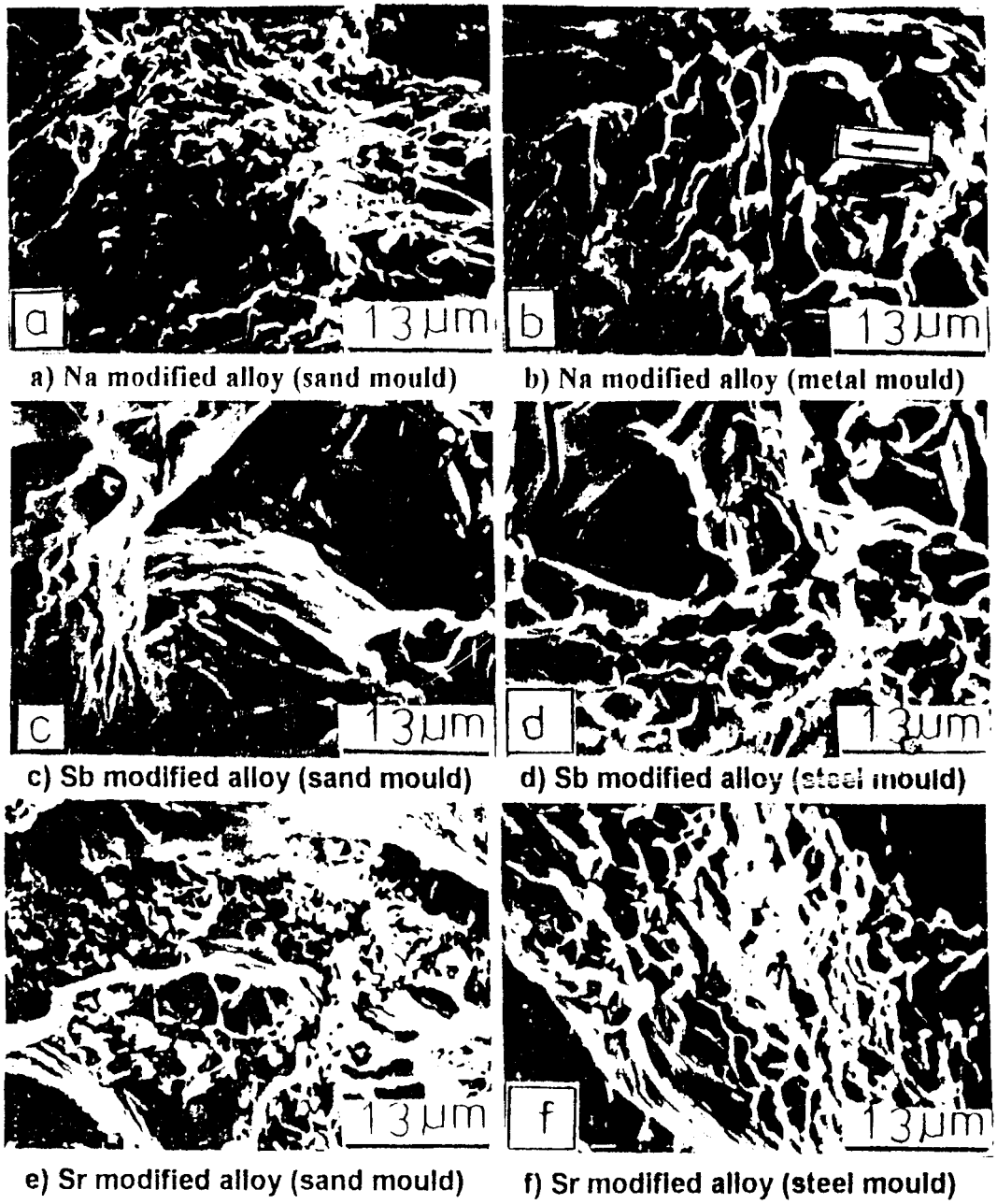

Figure 5 Features of the fracture surfaces of modified alloys as revealed by SEM.

hardness values of 400 to 500 HV (MPa) depending on the Si-content. The modified alloys showed almost the same hardness values as the non-modified alloys for the respective Si-contents. This phenomenon was valid for both sand and permanent-mould castings [38]. The hardness values obtained in the present study ranging from 445 to 460 HV (MPa) for the non-modified alloys, and from 448 to 491 HV (MPa) for the modified alloys correspond well with the hardness values reported above by Mondolfo for both non-modified and modified Al-Si alloys.

4.4. Tensile properties

An increase in tensile strength, ductility and toughness was observed due to modification (Table V). The increase in the tensile properties (σ_{pr}, E% and toughness) is shown in Table VI for the modified alloys. All the tensile properties of Sr-modified alloy are superior to others. It is interesting to note that the increases in tensile properties for Sr-modified sand cast alloy were higher by 12.7% for σ_{pr}, 16.3% for ductility, and 33.3% for toughness to that of Na-modified alloy. For metal mould ingots the increases were respectively: 16.7%, 32.5%, and 41%. It can be seen that the impact of modification on the tensile properties is more pronounced for the higher SCR (metal mould). Fig. 7 exhibits a comparison among the stress/plastic strain diagrams for the modified and non-modified alloys. Superiority of the tensile properties of Sr-modified alloy is that clearly demonstrated by curves 3 and 4 in Fig. 7. These values of the tensile properties confirm those reported by Mondolfo [38] for sand and metal mould ingots, although he did not mention the type of modifier used.

4.5. Fracture characteristics

The SEM fractographs presented in Fig. 4 characterise the nature of fracture in the non-modified version of the present alloy. Generally, features typical of

TABLE VI Percentage change of the tensile properties due to Na, Sb and Sr modification

		% increase w.r.t[a] nonmodified alloy			% change w.r.t Na modified alloy			% increase w.r.t Sb modified alloy		
Mould type	Modifier	σ_{pr}	E	Toughness	σ_{pr}	E	Toughness	σ_{pr}	E	Toughness
Sand	Na	48.6	207	314.9	—	—	—	10	16.2	5.4
	Sb	35.1	164	293.6	−9	−13.9	−5.1	—	—	—
	Sr	67.6	257	453.2	+12.7	+16.3	+33.3	24	35.1	40.5
Metal	Na	25.0	220	320	—	—	—	7.1	9.6	13.5
	Sb	16.7	192	270	−6.7	−8.7	−11.9	—	—	—
	Sr	45.8	324	495	+16.7	+32.5	+41.7	25	45.2	60.8

[a] w.r.t. with respect to.

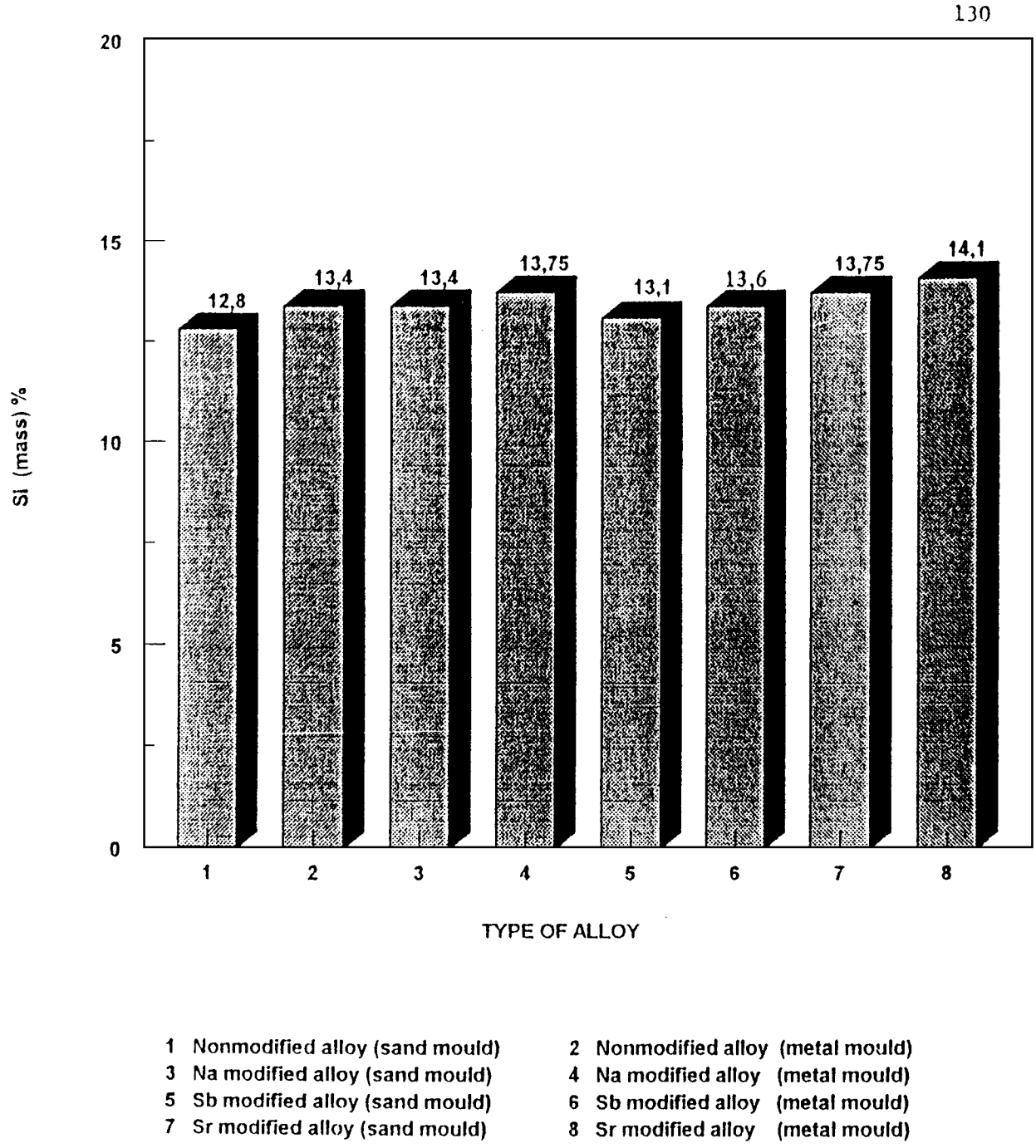

Figure 6 Effect of solidification cooling rate and Na, Sb and Sr modification on the shift of the eutectic point.

cleavage fracture could be identified. Thus, the fracture pattern shown in Fig. 4 can be rated as a typical brittle fracture. These features explain the poor tensile properties of the non-modified alloy (Table V and Fig. 7). The broken Si-particles detected on the fracture surface suggest that cracks be initiated in the Si-particles. It can thus be concluded that in non-modified alloys, where the Si-particles have a coarse plate-like

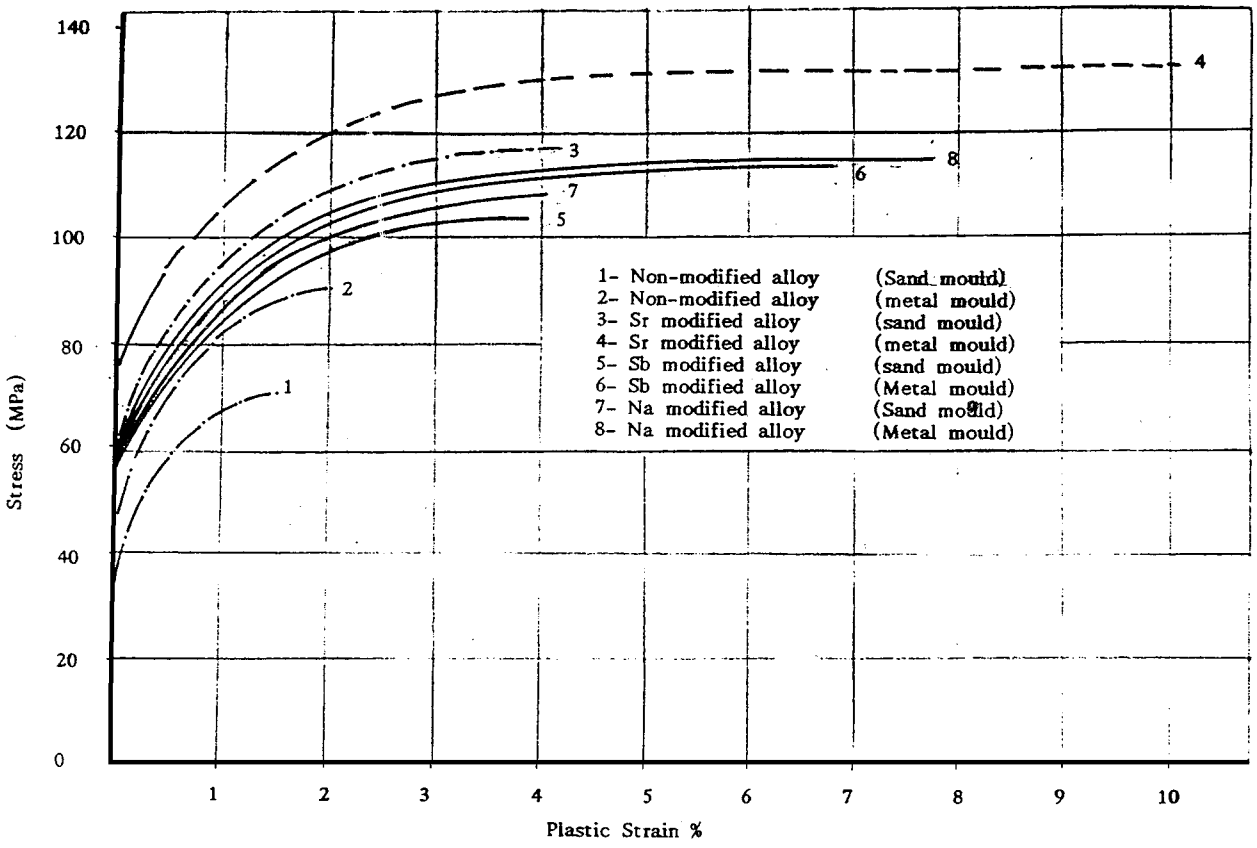

Figure 7 Comparison among the stress/plastic strain curves of Na, Sb and Sr modified alloys.

form, fracture initiation and propagation through these platelets is more likely to occur.

The fracture characteristics of Na-modified alloy described earlier in the article 3.4 and shown in Fig. 5a and b are great evidence that the eutectic-Si morphology influences significantly the fracture behaviour of the present alloy. The fracture mechanism changes from brittle (Fig. 4a and b) to ductile (Fig. 5a and b) due to the change of Si-particles shape from a plate-like to a fibrous form. The ripple pattern observed on the fracture surface (cf. Fig. 5a and b) suggests that a considerable amount of plastic deformation occurs, likely, prior to fracture.

The features of fracture surfaces of the Sb-modified alloy were presented in Fig. 5c and d. The mixed mode of fracture clearly shows that the fracture occurs by the growth of internal cavities and that cavity nucleation occurred around the Si-particles. The fracture pattern (brittle/ductile) seems to be determined by the Si-particle size and morphology, which may influence the damage initiation and the level of strain in the matrix-material [23].

Typical dimple and ripple patterns were observed on the fracture surfaces of the Sr-modified alloy (Fig. 5e and f). Therefore, the fracture in Sr-modified alloy can be rated as a ductile fracture. The light portions in Fig. 5a suggest that the Al-matrix takes part in the fracture process. It also tells that the fracture is preceded by plastic deformation. It is interesting to note that the dimple size is larger for metal mould ingots (Fig. 5f) than that of sand mould cast ingots (Fig. 5e). In addition to that, the dimple depth of the former is a smaller (shallower dimple). Large-size and shallow dimples reflect the higher ductility of the metal mould alloy studied (Table V).

The optical fractography of the longitudinal section near the fracture surfaces of Na, Sb, and Sr-modified alloys, which were shown in Fig. 3e and f, revealed that the crack preferred to propagate along the eutectic phase, circumventing the Al-dendrites. The dimple and smooth ripple patterns observed by SEM on the fracture surfaces of the Na and Sr-modified alloys (Fig. 5a, b, c and f) suggest a transgranular type of fracture across the grains of the eutectic matrix.

5. Conclusion

1. The eutectic-Si is found in different morphologies depending upon the presence or absence of the modifying agent and the type of the modifier used. Plate-like eutectic-Si characterises the non-modified alloys. Sb-modified version displays a lamellar eutectic-Si. Modification with Na or Sr resulted in changing the coarse plate-like morphology into a fine fibrous one.

2. Detection of the location of the eutectic-point on the phase-diagram has been carried out based on the determination of the volume fraction of the constituent phases. Modification resulted in shifting the eutectic-point to higher Si side at temperatures lower than that of the binary eutectic temperature (850 K).

3. High solidification cooling rate when combined with Sr-modification enhances the hardness of the Al-5.5%Si alloy. HV reached a value of 491 MPa, which represents an increase of about 6.7% with respect to the non-modified one.

4. The increase in the tensile properties of sand mould Sr-modified alloy compared to those of

Na-modified alloy were 12.7% for the proof stress. 16.3% for the ductility and 33.3 for the toughness. For metal mould ingots, the increases were 16.7%, 32.5% and 41.7% respectively.

5. The fracture characteristics were found to be strongly related to the microstructural features. For non-modified alloys, where the Si-particles have a coarse, plate-like form, the fracture pattern was of brittle appearance. The miniature lamellar structure of eutectic-Si in Sb-modified alloy resulted in a mixed mode of fracture (brittle/ductile). Typical ductile fracture (dimple + ripple) were found to be the characteristic of Na and Sr-modified alloys, with fibrous Si-particles.

6. An intergranular mode of fracture has been observed on the longitudinal section near the fracture surface of non-modified alloys. However, the dimple and smooth ripple patterns of fracture observed on the fracture surfaces of Na and Sr modified alloys suggest a transgranular fracture.

Acknowledgement

The authors would like to thank Prof. M. A. AlNawawy and Prof. S. ElGemae for their help and advice.

References

1. ASIM, Metals Handbook (Metals Park, Ohio, USA, 1948).
2. J. JORSTAD, *AFS Trans.* **92** (1984) 573.
3. B. THALL and B. CHALMERS, *J. Inst. Met.* **77** (1950) 79.
4. B. GUNTHER and H. JURGENS, *Giessesrel* **67**(1) (1980) 8.
5. K. RADHAKRISHNA, *Indian Foundry J.* **29** (1983) 115.
6. M. GIGLOTTI, *Metall. Trans.* **3** (1972) 933.
7. P. HESS and E. BLACKUMUN, *AFS Trans.* **83** (1975) 87.
8. J. CHARBONNIER, *AFS Int. Cast Met. J.* **4** (1979) 39.
9. S. HOLECEK and A. BRANDEJS, *Slevarents.* **1** (1979) 28.
10. N. GARAT, *Rev. Aluminium.* **49** (1979) 499.
11. Q. NAGEL and R. PORTALIER, *AFS Int. Cast Metals J.* **5** (1980) 2.
12. A. TELLI and S. KISAKUREK, *Scripta Metall.* **20** (1986) 1657.
13. M. HAQUE, *Met. Forum.* **6** (1983) 54.
14. *Idem., Foundry Trade. J.* **24** (1983) 387.
15. B. CLOSSET and J. GRUZLESKI, *Metall. Trans.* **13A** (1982) 945.
16. N. FATAHALLA, in Proc. of the 3rd Int. Conf. Cairo Univ., Cairo, Egypt, Dec. 28–30, 1985, edited by S. Bayoumi (Pergamon Press, 1985) p. 239.
17. N. FATAHALLA, *J. Mater. Sci.* **22** (1987) 1013.
18. *Idem.*, in Proc. of the 5th Int. Conf. on Mech. Behaviour of Mater., Beijin, China, 2, June 3–6, 1987, Vol. 2, p. 1419.
19. N. FATAHALLA, P. SECORDEL and M. SUERY, *J. Mater. Sci.* **23** (1988) 2419.
20. M. HAFIZ, T. KOBAYASHI and N. FATAHALLA, *Cast Metals J.* **7** (1994) 103.
21. N. FATAHALLA, "A Treatise on Materials Sci. and Eng.," (Al Ahram, Cairo, Egypt, 1995).
22. M. HAFIZ and T. KOBAYASHI, *Trans. J. Foundrymen's Society.* **1** (1993) 115.
23. *Idem., Scripta Metall. et Mater.* **31** (1994) 701.
24. M. HAFIZ, N. FATAHALLA and S. BAHI, *Z. Metallkde.* **81** (1990) 75.
25. N. FATAHALLA, *J. Mater. Sci.* **25** (1990) 3396.
26. *Idem., J. Mater. Sci.* **24** (1989) 2488.
27. M. HAFIZ, N. FATAHALLA and S. BAHI, in Proc. of the 2nd Int. Conf. Ain Shams Univ. on Production Eng. and Design for Development, Cairo, Egypt, Dec. 29–31, 1987, Vol. 2, p. 277.
28. ASM, Metals Handbook (Metals Park, Ohio, USA. 7, 1972) p. 241.
29. *Idem.*, (Metals Park, Ohio, USA. 9, 1985) p. 123.
30. S. SPEAR and G. GARDNER, *AFS Trans.* **71** (1963) 209.
31. G. SIGWORTH, *ibid.* **91** (1983) 7.
32. B. GALLOIS and G. SIGWORTH, in Proc. of the AFACMI Conf., USA, Dec. 11–12, 1984, p. 101.
33. A. HELLAWELL, "Progress in Mater. Sci.," (Pergamon Press, 15, 1970) p. 3.
34. V. RAUTA, in Proc. of the 2nd Int. Conf. on Molten Aluminium (AFS, 5, 1966) p. 396.
35. D. GRANGER, R. SAWTELL and M. KERSKER, *AFS Trans.* **92** (1984) 579.
36. W. LAORCHAN and J. GRUSLESKI, *ibid.* **100** (1992) 53.
37. A. HELLAWELL, "Progress in Mater. Sci.," (Pergamon Press, 22, 1977) p. 1.
38. L. MONDOLFO, "Aluminm Alloys: Structure and Properties," (Butterworth, England, 1976) p. 767.

Received 31 May 1995
and accepted 14 January 1999